

Importance Sampling via Score-based Generative Models

Heasung Kim, Taekyun Lee, Hyeji Kim, and Gustavo de Veciana

Department of Electrical and Computer Engineering
The University of Texas at Austin
Austin, TX 78712 USA

Abstract

Importance sampling, which involves sampling from a probability density function (PDF) proportional to the product of an importance weight function and a base PDF, is a powerful technique with applications in variance reduction, biased or customized sampling, data augmentation, and beyond. Inspired by the growing availability of score-based generative models (SGMs), we propose an entirely training-free Importance sampling framework that relies solely on an SGM for the base PDF. Our key innovation is realizing the importance sampling process as a backward diffusion process, expressed in terms of the score function of the base PDF and the specified importance weight function—both readily available—eliminating the need for any additional training. We conduct a thorough analysis demonstrating the method’s scalability and effectiveness across diverse datasets and tasks, including importance sampling for industrial and natural images with neural importance weight functions. The training-free aspect of our method is particularly compelling in real-world scenarios where a single base distribution underlies multiple biased sampling tasks, each requiring a different importance weight function. To the best of our knowledge our approach is the first importance sampling framework to achieve this.

1 Introduction

Score-based Generative Models (SGMs) have proven to be a very effective tool for sampling from high dimensional distributions [1, 2, 3]. Increasingly SGMs are being made available to capture a wide variety of data sets, including images [4, 5], audio [6, 7], and wireless environments [8, 9]. In this work, we consider the following problem: *Given an SGM, can we design a strategy for generating samples that satisfy pre-specified characteristics, e.g., samples corresponding to rare events or high losses on a downstream task?* Formally, this might be viewed as a form of importance sampling, where the aim is to generate representative “important” samples.

Mathematically, importance sampling is defined as follows: Consider a Probability Density Function (PDF) $p : \mathbb{R}^d \mapsto [0, 1]$ over the domain \mathbb{R}^d of the random vector \mathbf{X} , and importance weight function $l : \mathbb{R}^d \mapsto \mathbb{R}_+$ where \mathbb{R}_+ denotes the set of positive real values. The concept of importance sampling entails drawing samples from a modified PDF q , whose PDF is proportional to the product of the importance weight function l and the original PDF p . Formally, the importance sampling PDF is given by:

Preprint. Correspondence to: Heasung Kim <heasung.kim@utexas.edu>
Source code: <https://github.com/Heasung-Kim/importance-sampling-via-score-based-generative-models>

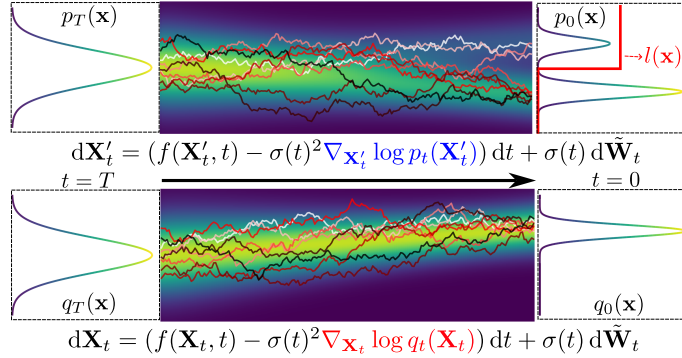


Figure 1: **Top**: Sampling process for $\mathbf{X}' \sim p(\mathbf{x})$. **Bottom**: Importance sampling process for $\mathbf{X} \sim q(\mathbf{x})$. The proposed method utilizes the pretrained $\nabla_{\mathbf{x}} \log p_t(\mathbf{x})$ and given importance weight function $l(\mathbf{x})$ to compute $\nabla_{\mathbf{x}} \log q_t(\mathbf{x})$ *without necessitating any additional training*.

Definition 1. (Importance Sampling PDF)

$$q(\mathbf{x}) = \frac{l(\mathbf{x})p(\mathbf{x})}{\int l(\mathbf{x})p(\mathbf{x}) d\mathbf{x}} \quad (1)$$

Importance sampling is a versatile technique with demonstrated effectiveness across various applications, including variance minimization in mean estimation, data augmentation, selective feature analysis, and bias and fairness considerations [10, 11, 12, 13].

In real-world scenarios, given a single base PDF $p(\mathbf{x})$ or samples drawn from it, we often seek to perform multiple importance sampling with different importance weight functions $l(\mathbf{x})$. For example, $l(\mathbf{x})$ can be designed to prioritize underrepresented classes, refining sampling to meet varying fairness criteria. Alternatively, $l(\mathbf{x})$ can represent a loss function, enabling the sampling of \mathbf{x} that induces high loss values. This allows for the identification of inputs associated with poor task model performance. Such flexibility highlights the power of importance sampling in addressing a wide range of practical challenges.

Despite its advantages, existing importance sampling methods face critical challenges: They typically require training or fine-tuning separate generative models for multiple importance sampling distributions corresponding to each and every weight function $l(\mathbf{x})$, a process that is computationally prohibitive and inefficient, particularly in scenarios involving multiple or dynamic importance weight functions. Therefore, we seek computationally efficient sampling methods that can adapt to multiple importance weight functions.

Contributions. The *main contribution* of this paper is the development of a novel approach to efficiently generate importance samples from a target distribution $q(\mathbf{x})$ given only the score function of the base distribution $p(\mathbf{x})$, without explicitly learning $q(\mathbf{x})$ or its score function. Our key innovation lies in deriving an approximate representation for the time-dependent score function of $q(\mathbf{x})$ in terms of the score function of $p(\mathbf{x})$ and the weight function $l(\mathbf{x})$ (Sec. 3). This approximation allows us to model the importance sampling process as a backward diffusion process, which *does not require any additional training of generative models*. To the best of our knowledge, this is the first

score-based importance sampling framework that does not require direct training of the importance sampling PDF or its score function.

Fig. 1 conceptually illustrates two backward diffusion processes. The first (top) transitions from a Gaussian distribution to a bimodal base PDF using the score function $\nabla_{\mathbf{x}} \log p_t(\mathbf{x})$. The second (bottom) depicts an importance sampling process targeting a single-peaked PDF (shaped by the importance weight $l(\mathbf{x})$), requiring $\nabla_{\mathbf{x}} \log q_t(\mathbf{x})$. Instead of learning $\nabla_{\mathbf{x}} \log q_t(\mathbf{x})$, we approximate it in terms of $\nabla_{\mathbf{x}} \log p_t(\mathbf{x})$ and $l(\mathbf{x})$, effectively leveraging the accessible and known quantities, making our approach training-free and scalable.

Theoretical Development. We provide a detailed derivation of how training-free importance sampling is achieved and conduct a technical analysis of the approximation accuracy within the proposed framework (Sec. 3).

Empirical Validation. We thoroughly evaluate the sampling accuracy by assessing how well our generated importance samples approximate the target importance sampling distribution across various synthetic scenarios (Sec. 4.1).

Applications. The versatility of our approach enables importance sampling for *any differentiable importance weight function* $l(\mathbf{x})$, including those modeled as neural networks. This allows us to address several challenging sampling tasks that existing importance sampling methods struggle to handle efficiently, such as: Designing $l(\mathbf{x})$ as a distortion measure computed by a neural autoencoder for a specific downstream task, enabling the targeted sampling of high-distortion-inducing instances (Sec. 4.2); Utilizing a neural classifier as $l(\mathbf{x})$ to enable training-free, dynamic class-wise bias/uniformity sampling, even in *SGMs that have never been trained with class labels* (Sec. 4.3-1); Defining $l(\mathbf{x})$ based on image characteristics, such as color or frequency emphasis, to sample images with desired attributes—achieving a new level of sampling control beyond traditional prompt conditioning (Sec. 4.3-2)

These results underscore the scalability and adaptability of our method, positioning it as a powerful and generalizable approach for importance sampling in SGMs.

Clarifying the Scope of Work. We state that our work is *fundamentally distinct* from conditional sampling with SGMs [14, 15] and methods refining SGMs to improve output quality, such as [16]. Conditional sampling typically involves training SGMs with conditions, whereas our approach focuses on training-free importance sampling with an *externally defined* importance weight function that operates independently of the original distribution. This also differs from approaches refining diffusion processes using trained discriminators to enhance SGM outputs or solve inverse problems [17, 18, 19]. Additionally, prior work applied SGMs to annealed importance sampling for variance reduction in distribution estimation [20], whereas we recover the importance sampling for an independently defined importance weight function—tackling an entirely different problem.

2 Background on SGM

The score-based generative modeling approaches aim to learn the score function of the target data distribution, $\nabla_{\mathbf{x}} \log q(\mathbf{x})$. This is achieved through a parameterized model, typically implemented as a neural network, to approximate the true score function. A notable innovation in score-based

generative modeling is the use of score functions for noise-perturbed data rather than relying solely on the score function of the original PDF. Learning the score function of noise-perturbed data enables the modeling of data generation as a Stochastic Differential Equation (SDE) and also leads to more robust training of the score function [3]. Specifically, a continuous-time noise perturbation process, or diffusion process, can be represented by the following SDE.

$$d\mathbf{X}_t = f(\mathbf{X}_t, t) dt + \sigma(t) d\mathbf{W}_t, \quad (2)$$

where $\mathbf{X}_0 \sim q(\mathbf{x})$, implying that \mathbf{X}_t at $t = 0$ follows the target distribution we aim to learn. In this context, $f : \mathbb{R}^d \times [0, T] \mapsto \mathbb{R}^d$ represents the drift coefficient, $\sigma(t) : [0, T] \mapsto \mathbb{R}$ denotes the diffusion coefficient, and $d\mathbf{W}_t$ indicates multidimensional Brownian motion. As time t progresses, the distribution of \mathbf{X}_t evolves, which we denote as $q_t(\mathbf{x})$.

When the score function $\nabla_{\mathbf{x}} \log q_t(\mathbf{x})$ is known, this framework enables sampling of \mathbf{X}_0 that follows PDF $q_0 = q$ via a corresponding backward SDE [21] which is given by

$$d\mathbf{X}_t = b_1(\mathbf{X}_t, t) dt + \sigma(t) d\tilde{\mathbf{W}}_t, \quad (3)$$

where $b_1(\mathbf{x}, t) = f(\mathbf{x}, t) - \sigma(t)^2 \nabla_{\mathbf{x}} \log q_t(\mathbf{x})$

with $\mathbf{X}_t \sim q_t$ and $d\tilde{\mathbf{W}}_t$ denoting the Brownian motion associated with the reverse-time process. For instance, given an initial sample $\mathbf{X}_T \sim q_T(\mathbf{x})$, solving SDE (3) yields a sample \mathbf{X}_0 with distribution q_0 . Typically, for sufficiently large values of T , a realization \mathbf{x}_T can be initialized as Gaussian noise.

Following convention [1, 22, 23, 24], we consider the following drift and diffusion coefficients,

$$f(\mathbf{x}, t) = -\frac{1}{2}\beta(t)\mathbf{x} \quad \text{and} \quad \sigma(t) = \sqrt{\beta(t)}$$

where $\beta(t)$ is a predefined scalar-valued continuous function such that $0 \leq \beta(t) \leq 1$. Here, in defining $\sigma(t)$ and $f(\mathbf{x}, t)$, we apply a slight abuse of notation: the scalar-vector multiplication in this context represents the elementwise multiplication of the vector by the scalar.

Notation. The symbol d denotes an infinitesimal increment. $\|\cdot\|$ indicates the spectral norm for matrices and the Euclidean (L_2) norm for vectors. We denote Gaussian and Uniform distributions by \mathcal{N} and \mathcal{U} .

3 Importance Sampling via SGM (ISSGM)

3.1 Problem Formulation

Given an SGM that models a base distribution $p(\mathbf{x})$ and a desired weight function $l(\mathbf{x})$, our ultimate goal is to devise an algorithm that can draw samples from the importance sampling PDF $q(\mathbf{x}) = \frac{l(\mathbf{x})p(\mathbf{x})}{\int l(\mathbf{x})p(\mathbf{x}) d\mathbf{x}}$, where l is a positive function as $l(\mathbf{x}) \geq m$ and $m > 0$. We assume that the logarithms of p, q, l are twice continuously differentiable with respect to \mathbf{x} .

3.2 Proposed method

We introduce a novel approach for generating importance samples, following $q(\mathbf{x})$, using an SGM trained on the base distribution $p(\mathbf{x})$. Notably, our method neither requires a single sample from the distribution $q(\mathbf{x})$ (or $p(\mathbf{x})$) nor necessitates any additional retraining.

Key Idea. We first show that the time-dependent score function for the importance sampling PDF, denoted as $\nabla_{\mathbf{x}} \log \tilde{q}_t(\mathbf{x}) \approx \nabla_{\mathbf{x}} \log q_t(\mathbf{x})$, can be approximated in terms of the score function for the base PDF, $\nabla_{\mathbf{x}} \log p_t(\mathbf{x})$ and the target weight function $l(\mathbf{x})$, both of which are readily available. Importantly, this approximation is computationally simple and requires no additional training. We further show that the approximation error vanishes as $t \rightarrow 0$ under mild assumptions. Next, we perform the backward SDE in (3) with the approximated score function as:

$$d\mathbf{X}_t = \beta(t) \left[\frac{-\mathbf{X}_t}{2} - \nabla_{\mathbf{x}_t} \log \tilde{q}_t(\mathbf{X}_t) \right] dt + \sqrt{\beta(t)} d\tilde{\mathbf{W}}_t, \quad (4)$$

through which we generate importance samples.

Our approach offers two major advantages: (a) it renders the *importance sampling process training-free*, thereby eliminating the need to learn the PDF q or score function of q , and (b) it enhances the *scalability and adaptability* of the algorithm, as it relies solely on the inference of readily available quantities, $\nabla_{\mathbf{x}} \log p_t(\mathbf{x})$ and $l(\mathbf{x})$.

Derivation of the Proposed SDE (4). We aim to represent $\nabla_{\mathbf{x}} \log q_t(\mathbf{x})$ in terms of $\nabla_{\mathbf{x}} \log p_t(\mathbf{x})$ and $\nabla_{\mathbf{x}} \log l(\mathbf{x})$. To achieve this, we begin by examining the form of the importance sampling distribution for the noise-perturbed importance samples, $q_t(\mathbf{x})$, under the SDE defined in (2). Consider the transition probability density function $G : \mathbb{R}^d \times \mathbb{R}^d \times [0, T] \mapsto \mathbb{R}_+$, also referred to as the Green's function or fundamental solution of the SDE [25, 26, 27]. This function represents the probability density of the process transitioning from the given initial state $\mathbf{X}_0 = \mathbf{y}$ to the state \mathbf{x} at time t . Specifically, $G(\mathbf{x}, \mathbf{y}, t)$ denotes the probability density of transitioning from \mathbf{y} to \mathbf{x} over time t . Using this Green's function, we can express $q_t(\mathbf{x})$ as

$$q_t(\mathbf{x}) = \int G(\mathbf{x}, \mathbf{y}, t) q_0(\mathbf{y}) d\mathbf{y} \quad (5)$$

$$= \frac{1}{Z_0} \int G(\mathbf{x}, \mathbf{y}, t) l(\mathbf{y}) p_0(\mathbf{y}) d\mathbf{y} \quad (6)$$

where $q_0 = q$, $p_0 = p$, and Z_0 is the normalization constant, $Z_0 = \int l(\mathbf{x}) p(\mathbf{x}) d\mathbf{x}$ as given in (1).

To further investigate the relationship between q_t and p_t , we consider an SDE of $\mathbf{X}'_t \in \mathbb{R}^d$, which shares the same drift and diffusion coefficients as in (2), but where the initial distribution is $p_0 = p$ rather than q_0 :

$$d\mathbf{X}'_t = -\frac{1}{2}\beta(t)\mathbf{X}'_t dt + \sqrt{\beta(t)} d\mathbf{W}_t, \quad (7)$$

where $\mathbf{X}'_0 \sim p_0$. It should be noted that the corresponding Green's function for this SDE is also G in (5), and the distribution of \mathbf{X}' at time t , denoted by p_t , is given as follows

$$p_t(\mathbf{x}) = \int G(\mathbf{x}, \mathbf{y}, t) p_0(\mathbf{y}) d\mathbf{y}. \quad (8)$$

By using (6) and (8), we have

$$q_t(\mathbf{x}) = \frac{p_t(\mathbf{x})}{Z_0} \int l(\mathbf{y}) G(\mathbf{x}, \mathbf{y}, t) \frac{p_0(\mathbf{y})}{p_t(\mathbf{x})} d\mathbf{y} = \frac{p_t(\mathbf{x})}{Z_0} \mathbb{E}_{\mathbf{X}'_0 \sim p_{\mathbf{X}'_0 | \mathbf{X}'_t}(\cdot | \mathbf{x})} [l(\mathbf{X}'_0)] \quad (9)$$

where $p_{\mathbf{X}'_0 | \mathbf{X}'_t}(\cdot | \mathbf{x})$ is the conditional PDF of the initial state \mathbf{X}'_0 for a given state $\mathbf{X}'_t = \mathbf{x}$ at t under the SDE given in (7).

We can observe that q_t can be represented in terms of p_t and l as shown in (9). Consequently, the score function for importance sampling can be represented as

$$\nabla_{\mathbf{x}} \log q_t(\mathbf{x}) = \nabla_{\mathbf{x}} \log p_t(\mathbf{x}) + \nabla_{\mathbf{x}} \log \mathbb{E}_{\mathbf{X}'_0 \sim p_{\mathbf{X}'_0|\mathbf{X}'_t}(\cdot|\mathbf{x})} [l(\mathbf{X}'_0)]. \quad (10)$$

For practical computation of (10), we consider the first order Taylor approximation of $l(\mathbf{X}'_0)$ at $\bar{\mathbf{x}}'_0|_{\mathbf{x},t} := \mathbb{E}[\mathbf{X}'_0|\mathbf{X}'_t = \mathbf{x}]$ which gives us

$$l(\mathbf{X}'_0) \approx l(\bar{\mathbf{x}}'_0|_{\mathbf{x},t}) + \nabla l(\bar{\mathbf{x}}'_0|_{\mathbf{x},t})^\top (\mathbf{X}'_0 - \bar{\mathbf{x}}'_0|_{\mathbf{x},t}). \quad (11)$$

Substituting (11) to (10), we have

$$\nabla_{\mathbf{x}} \log q_t(\mathbf{x}) \approx \nabla_{\mathbf{x}} \log p_t(\mathbf{x}) + \nabla_{\mathbf{x}} \log l(\bar{\mathbf{x}}'_0|_{\mathbf{x},t}). \quad (12)$$

Note that $\bar{\mathbf{x}}'_0|_{\mathbf{x},t}$ is the conditional mean of the initial state for a given \mathbf{x} at t and can be obtained through the Tweedie's approach ([28, 29, 19]) as

$$\bar{\mathbf{x}}'_0|_{\mathbf{x},t} = \frac{1}{\sqrt{\bar{\alpha}(t)}} (\mathbf{x} + (1 - \bar{\alpha}(t)) \nabla_{\mathbf{x}} \log p_t(\mathbf{x})) \quad (13)$$

where $\bar{\alpha}(t) = \exp\left(-\int_0^t \beta(s) ds\right)$.

Given that we now have a tractable form for $\nabla_{\mathbf{x}} \log l(\bar{\mathbf{x}}'_0|_{\mathbf{x},t})$ by (13), we can apply the chain rule to represent $\nabla_{\mathbf{x}} \log l(\bar{\mathbf{x}}'_0|_{\mathbf{x},t})$ as follows

$$\nabla_{\mathbf{x}} \log l(\bar{\mathbf{x}}'_0|_{\mathbf{x},t}) = \frac{(\mathbf{I} + (1 - \bar{\alpha}(t)) H_{p_t}(\mathbf{x}))}{\sqrt{\bar{\alpha}(t)}} \nabla_{\bar{\mathbf{x}}'_0|_{\mathbf{x},t}} \log l(\bar{\mathbf{x}}'_0|_{\mathbf{x},t}) \quad (14)$$

where $H_{p_t}(\mathbf{x})$ is the Hessian matrix of $\log p_t(\mathbf{x})$.

To enhance the practicality of the proposed method, we approximate the Hessian matrix-vector multiplication in (14) by the first-order Taylor's approximation with a sufficiently small $\epsilon > 0$ as

$$\begin{aligned} \nabla_{\mathbf{x}} \log p_t(\mathbf{x}) + \epsilon H_{p_t}(\mathbf{x}) \nabla_{\bar{\mathbf{x}}'_0|_{\mathbf{x},t}} \log l(\bar{\mathbf{x}}'_0|_{\mathbf{x},t}) \\ \approx \nabla_{\mathbf{x}} \log p_t(\mathbf{x} + \epsilon \nabla_{\bar{\mathbf{x}}'_0|_{\mathbf{x},t}} \log l(\bar{\mathbf{x}}'_0|_{\mathbf{x},t})). \end{aligned} \quad (15)$$

Combining (3), (12), and (15), we finally suggest to use the following approximated score function.

$$\begin{aligned} \nabla_{\mathbf{x}} \log \tilde{q}_t(\mathbf{x}) := \nabla_{\mathbf{x}} \log p_t(\mathbf{x}) + \frac{\nabla_{\bar{\mathbf{x}}'_0|_{\mathbf{x},t}} \log l(\bar{\mathbf{x}}'_0|_{\mathbf{x},t})}{\sqrt{\bar{\alpha}(t)}} \\ + \frac{\nabla_{\mathbf{x}} \log p_t(\mathbf{x} + \epsilon \nabla_{\bar{\mathbf{x}}'_0|_{\mathbf{x},t}} \log l(\bar{\mathbf{x}}'_0|_{\mathbf{x},t})) - \nabla_{\mathbf{x}} \log p_t(\mathbf{x})}{\epsilon(1 - \bar{\alpha}(t))^{-1} \sqrt{\bar{\alpha}(t)}} \end{aligned}$$

whose corresponding backward SDE to sample $\mathbf{X} \sim q_0$ is given as

$$\begin{aligned} d\mathbf{X}_t &= -\frac{\beta(t)}{2} [\mathbf{X}_t + 2\nabla_{\mathbf{x}_t} \log \tilde{q}_t(\mathbf{X}_t)] dt + \sqrt{\beta(t)} d\tilde{\mathbf{W}}_t \\ &= \left[-\frac{1}{2} \beta(t) \mathbf{X}_t - \beta(t) \nabla_{\mathbf{x}_t} \log p_t(\mathbf{X}_t) \right] dt + \sqrt{\beta(t)} d\tilde{\mathbf{W}}_t \\ &\quad - \beta(t) \left[\frac{\nabla_{\bar{\mathbf{x}}'_0|_{\mathbf{x}_t,t}} \log l(\bar{\mathbf{x}}'_0|_{\mathbf{x}_t,t})}{\sqrt{\bar{\alpha}(t)}} - \frac{\nabla_{\mathbf{x}_t} \log p_t(\mathbf{X}_t)}{\epsilon(1 - \bar{\alpha}(t))^{-1} \sqrt{\bar{\alpha}(t)}} + \frac{\nabla_{\mathbf{x}_t} \log p_t(\mathbf{X}_t + \epsilon \nabla_{\bar{\mathbf{x}}'_0|_{\mathbf{x}_t,t}} \log l(\bar{\mathbf{x}}'_0|_{\mathbf{x}_t,t}))}{\epsilon(1 - \bar{\alpha}(t))^{-1} \sqrt{\bar{\alpha}(t)}} \right] dt. \end{aligned} \quad (16)$$

This proposed SDE (16) can be solved by the Euler–Maruyama method [30], i.e., iterative discretization of the SDE. We reiterate and further elaborate on the key benefits of our approach for generating importance samples as follows.

Remark 1 (Training-Free Importance Sampling). The proposed backward SDE in (16) demonstrates that, for a given score function $\nabla_{\mathbf{x}} \log p_t(\mathbf{x})$ and importance weight function $l(\mathbf{x})$, *importance sampling can be approximated without additional training*. This presents a substantial advantage over existing methods, which require learning the density of q through individual training for each specific l .

In modern applications, pre-trained score functions are widely available [15, 31, 32] and can be directly leveraged. Our approach enables the direct application of importance sampling with any differentiable importance weight function $l(\mathbf{x})$, thereby eliminating the need for further training.

Remark 2 (High Scalability and Applicability). The proposed method requires only the score function of the original PDF and the differentiable function l , enabling diverse advanced importance measures, particularly those implemented via differentiable neural networks. For example, in a neural autoencoder designed to compress input instances, the importance weight for each instance could be defined by the compression-induced distortion, thereby prioritizing high-distortion samples. Applying the proposed algorithm in this context allows for targeted sampling of instances prone to high distortion, aiding in feature analysis focused on the high-distortion cases.

Computational Complexity. The additional computational cost introduced by our approach, compared to the base score-based sampling, is minimal. Calculating $\bar{\mathbf{x}}'_0|_{\mathbf{x},t}$ involves only a linear transformation of \mathbf{x} and the precomputed score function, as outlined in (13). Aside from this negligible cost, the potential overhead is the computation of $\nabla_{\bar{\mathbf{x}}'_0|_{\mathbf{x},t}} \log l(\bar{\mathbf{x}}'_0|_{\mathbf{x},t})$ to evaluate the final term in (16). This is efficiently achieved with a single gradient backpropagation step on l with respect to the realization $\bar{\mathbf{x}}'_0|_{\mathbf{x},t}$ and one inference step of the score function. Overall, this additional cost is *significantly less demanding* than methods requiring exact PDF or score function for each individual $l(\mathbf{x})$.

3.3 Theoretical Analysis

In this section, we establish Theorem 1 providing an upper bound on the Euclidean norm discrepancy between the proposed approximated score function and the true score function.

Assumption 1. (Bounded derivatives of $\log l(\mathbf{x})$) For all $\mathbf{x} \in \mathbb{R}^d$ and $t \in [0, T]$, we have $\|\nabla_{\mathbf{x}} \log l(\mathbf{x})\| \leq \eta_1$, $\|H_l(\bar{\mathbf{x}}'_0|_{\mathbf{x},t})\| \leq \eta_2$, and $\|\partial H_l(\bar{\mathbf{x}}'_0|_{\mathbf{x},t})/\partial \mathbf{x}\|_F \leq \eta_F$, where $H_l(\mathbf{x})$ is Hessian matrix of $\log l(\mathbf{x})$.

Assumption 1 implies that the importance weight function’s log-derivatives remain finite. Recall that we consider a strictly positive importance weight function $l(\mathbf{x}) > 0$, which reasonably supports the assumption of bounded log derivatives, avoiding unbounded behavior.

Assumption 2. (Bounded log PDF derivatives) For all $\mathbf{x}, \mathbf{y} \in \mathbb{R}^d$ and $t \in [0, T]$, we have $\|\nabla_{\mathbf{x}} \log p_{\mathbf{x}'_0|_{\mathbf{x}'_t}}(\mathbf{y}|\mathbf{x})\| \leq \gamma_t$, $\|H_{p_t}(\mathbf{x})\| \leq \zeta_t$, and $\|H_{p_t}(\mathbf{x}) - H_{p_t}(\mathbf{y})\| \leq L_t \|\mathbf{x} - \mathbf{y}\|$.

The bounded norm of the score function and Hessian of the log-likelihood are standard assumptions in the analysis of SGMs [33, 34, 35, 36]. The Lipschitz continuity of the Hessian often holds under a bounded Hessian assumption [35], especially in practical implementations of SGMs where the domain is often compact [1, 2] with high probability.

Theorem 1. (Score function gap) *Suppose that Assumptions 1–2 hold and for all $\mathbf{x} \in \mathbb{R}^d$ and $t \in [0, T]$, the importance weight function l is approximately equal to its second-order Taylor expansion at the estimated mean as $l(\mathbf{X}'_0) \cong l(\bar{\mathbf{x}}'_0|\mathbf{x},t) + \nabla l(\bar{\mathbf{x}}'_0|\mathbf{x},t)^\top (\mathbf{X}'_0 - \bar{\mathbf{x}}'_0|\mathbf{x},t) + \frac{1}{2} (\mathbf{X}'_0 - \bar{\mathbf{x}}'_0|\mathbf{x},t)^\top H_t(\bar{\mathbf{x}}'_0|\mathbf{x},t) (\mathbf{X}'_0 - \bar{\mathbf{x}}'_0|\mathbf{x},t)$.*

For a given $\epsilon > 0$, the gap between the true score function of the importance sampling PDF and the approximated score function is upper-bounded as

$$\|\nabla_{\mathbf{x}} \log q_t(\mathbf{x}) - \nabla_{\mathbf{x}} \log \tilde{q}_t(\mathbf{x})\| \leq \frac{(1 - \bar{\alpha}(t))L_t\eta^2\epsilon}{2\sqrt{\bar{\alpha}(t)}} + \lambda_t \mathbb{E} [\|\mathbf{X}'_0 - \bar{\mathbf{x}}'_0|\mathbf{x},t\|^2 | \mathbf{X}'_t = \mathbf{x}] \quad (17)$$

where $\lambda_t = \frac{1}{2m}(\eta_F + \gamma_t\eta_2) + \frac{(1+(1-\bar{\alpha}(t))\zeta_t)\eta\eta_2}{2m^2\sqrt{\bar{\alpha}(t)}}$.

Remark 3 (Bounded score function gap by variance). The gap between the true score function and the proposed approximation is bounded by $\mathbb{E} [\|\mathbf{X}'_0 - \bar{\mathbf{x}}'_0|\mathbf{x},t\|^2 | \mathbf{X}'_t = \mathbf{x}]$, which is the *trace of the covariance matrix of \mathbf{X}'_0 whose PDF is conditioned on the observation \mathbf{x} at t* . As $t \rightarrow 0$, this conditional variance converges to zero resulting the second term on the right-hand side of (17) vanishes, making the gap negligible. Additionally, the first term, $\frac{(1-\bar{\alpha}(t))L_t\eta^2\epsilon}{2\sqrt{\bar{\alpha}(t)}}$, also approaches 0 as $\bar{\alpha}(t) \rightarrow 1$ when $t \rightarrow 0$.

4 Experiments

4.1 Importance Sampling Performance Analysis

In this section, we evaluate the proposed method by measuring the ‘distance’ between the ground truth importance sampling distribution and the sample distribution generated by our approach across various scenarios. No prior baselines exist for our setup (i.e., we have access only to an SGM). Nevertheless, establishing a baseline—particularly a generative model-driven approach—would be valuable. Thus we parameterize the importance sampling distribution with state-of-the-art (SOTA) density-based generative models, optimized via Cross Entropy Minimization (CEM) method [37] using only samples from the base distribution p . Our method is applied to the same dataset, ensuring both approaches use an equal number of samples.

It is important to note that a direct comparison with this baseline is inherently unfair due to fundamental differences in mechanism. The baseline requires extensive neural network training with substantial hyperparameter tuning, whereas our approach remains ***the first score-based, training-free importance sampling framework*** that accommodates a broad range of *externally defined importance weight functions* $l(\mathbf{x})$. Here, “training-free” signifies that, given an SGM for the base distribution, our method operates without training an additional generative model specific to $l(\mathbf{x})$.

Setup. We shall initially consider the Circles, Spiral, Pinwheel, and 8-Gaussians (8-G) datasets [38, 39] with two different importance weight functions $l_1(\mathbf{x}) = \|\mathbf{x}\|^2$ and $l_2(\mathbf{x}) = \sum_{i \in [d]} [\mathbf{x}]_i + 2$, i.e., Euclidean norm square and element summation.

Evaluation metrics. The use of these closed-form data distributions and importance weight functions enable us to recover the optimal importance sampling distribution via the accept/reject method, facilitating the evaluation of importance sampling performance based on the Jensen-Shannon

Table 1: Performance comparison. (✓) represents a training-free algorithm, whereas (✗) indicates an algorithm requiring training for each $l(\mathbf{x})$. Metric: Jensen–Shannon divergence to ground truth importance sampling distribution, with lower values indicating better performance.

	Circles, l_1	Circles, l_2	Spiral, l_1	Spiral, l_2
MADE-MAA (✗)	0.209 ± 1e-3	0.292 ± 8e-4	0.154 ± 3e-2	0.119 ± 2e-1
NIS (✗)	0.122 ± 4e-4	0.123 ± 2e-4	0.096 ± 5e-5	0.227 ± 4e-3
NSF (✗)	0.121 ± 7e-4	0.121 ± 1e-3	0.097 ± 1e-4	0.100 ± 6e-3
CSF (✗)	0.121 ± 3e-4	0.121 ± 7e-4	0.094 ± 4e-2	0.102 ± 1e-3
TNA (✗)	0.129 ± 3e-4	0.137 ± 6e-3	0.201 ± 9e-4	0.228 ± 5e-3
ISSGM (Ours, ✓)	0.117 ± 2e-4	0.121 ± 3e-4	0.107 ± 1e-4	0.106 ± 5e-3
	Pinwheel, l_1	Pinwheel, l_2	8-G, l_1	8-G, l_2
MADE-MAA (✗)	0.174 ± 2e-1	0.128 ± 2e-3	0.215 ± 4e-2	0.155 ± 2e-3
NIS (✗)	0.120 ± 8e-4	0.106 ± 2e-3	0.105 ± 2e-3	0.106 ± 1e-4
NSF (✗)	0.117 ± 1e-3	0.104 ± 4e-4	0.108 ± 1e-4	0.108 ± 3e-4
CSF (✗)	0.117 ± 2e-3	0.104 ± 2e-2	0.108 ± 6e-4	0.108 ± 3e-2
TNA (✗)	0.118 ± 4e-3	0.107 ± 8e-3	0.156 ± 9e-4	0.127 ± 2e-2
ISSGM (Ours, ✓)	0.123 ± 1e-2	0.103 ± 6e-4	0.104 ± 6e-4	0.104 ± 1e-4

Divergence [40] – this is a symmetric variant of the Kullback-Leibler divergence, i.e., the distance between estimated samples and the optimal importance sampling distribution.

Our method. We use Denoising Diffusion Probabilistic Models (DDPM) [1] to obtain the base score function, and use the SDE discretization method.

Baselines. We adopt the following representative and SOTA density estimation-based generative models: Masked Autoencoder for Distribution Estimation [41] combined with the Masked Affine Autoregressive technique (MADE-MAA) [42], implemented using a density flow model with CEM; leveraging the Piecewise Quadratic Coupling Transform proposed in Neural Importance Sampling (NIS) [43]; Neural Spline Flows (NSF) [44] which utilize spline transformations to model complex distributions; Cubic Spline Flow [45] (CSF); and Transformer Neural Autoregressive density estimation method (TNA), incorporating masked autoregressive multi-head attention [46].

Results. In Table 4.1, we present the performance evaluation of the proposed importance sampling method. Our approach achieves the best performance in 5 out of 8 scenarios. We stress that for the two given importance weight functions, our method requires only a single base score function training. Even in cases where the proposed importance sampling does not attain the best performance, the gap remains marginal, with the Jensen-Shannon divergence difference being less than 0.015. This highlights the robustness of our approach. By contrast, some of our baselines exhibit significant performance variation across the considered scenarios. For instance, while TNA achieves performance comparable to the best-performing method in the Pinwheel scenario, its performance deteriorates significantly on the Spiral dataset, where its divergence metric is twice that of the best approach.

Fig. 2 exhibits a visualization of a base sampling and the importance sampling processes for the Spiral distribution with the norm squared weight. The top row shows the sampling process for $\mathbf{X}' \sim p$ based on depicting the evolution of distribution of $\mathbb{E}[\mathbf{X}'_0 | \mathbf{X}'_t]$. The bottom row shows our proposed importance sampling method for $\mathbf{X} \sim q$ by exhibiting the evolution of the distribution of $\mathbb{E}[\mathbf{X}_0 | \mathbf{X}_t]$. Note that at $t = 0$ (rightmost column), *the distributions of the conditional means correspond to $p(\mathbf{x})$ and $q(\mathbf{x})$ respectively.*

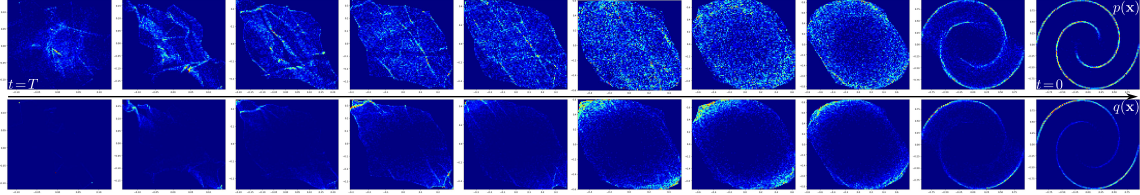


Figure 2: **Top row**: sampling process for $\mathbf{X}' \sim p(\mathbf{x})$. **Bottom row**: proposed importance sampling process for $\mathbf{X} \sim q(\mathbf{x})$. From left to right, each column corresponds to $t = 500, 400, \dots, 0$, showing the distributions of $\mathbb{E}[\mathbf{X}'_0 | \mathbf{X}'_t]$ and $\mathbb{E}[\mathbf{X}_0 | \mathbf{X}_t]$. Thus, the rightmost column illustrates the PDFs $p(\mathbf{x})$ (top) and $q(\mathbf{x})$ (bottom). The proposed approach enables efficient *importance sampling on the correct spiral-shaped manifold without any additional training for $l(\mathbf{x})$* , selectively emphasizing instances with a high norm with $l(\mathbf{x}) = \|\mathbf{x}\|^2$.

Table 2: Importance weight functions and importance values.

Experiment, $l(\mathbf{x})$	$\mathbb{E}_{\mathbf{X}' \sim p}[l(\mathbf{X}')]$	$\mathbb{E}_{\mathbf{X} \sim q}[l(\mathbf{X})]$ (Ours)
Fig. 2, Spiral, $\ \mathbf{x}\ ^2$	6.75×10^{-1}	8.55×10^{-1}
Fig. 3, CSI, $D(F_{\text{dec}}(F_{\text{enc}}(\mathbf{x})), \mathbf{x})$	3.07×10^{-4}	6.09×10^{-4}
Fig. 4, CelebA, a classifier	3.51×10^{-1}	5.12×10^{-1}
Fig. 5, StableCascade, a frequency analyzer	1.36	4.39

For every t , we compute the mean by using Tweedie’s formula $\frac{1}{\sqrt{\bar{\alpha}(t)}}(\mathbf{x}_t + (1 - \bar{\alpha}(t))\nabla_{\mathbf{x}_t} \log p_t(\mathbf{x}_t))$ for the original sampling process and $\frac{1}{\sqrt{\bar{\alpha}(t)}}(\mathbf{x}_t + (1 - \bar{\alpha}(t))\nabla_{\mathbf{x}_t} \log \tilde{q}_t(\mathbf{x}_t))$ for our importance sampling approach. We present 2D histograms for each time step, where reddish pixels indicate high probability density and blue pixels represent lower density. The histograms on the far right, corresponding to $t=0$, illustrate the PDFs, p (top) and q (bottom), as $\bar{\alpha}(0)=1$.

The results show that our proposed method performs importance sampling over the *feasible manifold*, i.e., the domain where $p(\mathbf{x}) \neq 0$; and reflects the specified importance weight function l , by resulting in higher densities for instances with high l values. Importantly, this approach leverages $\nabla_{\mathbf{x}} \log p_t(\mathbf{x})$ to approximate $\nabla_{\mathbf{x}} \log q_t(\mathbf{x})$ without any additional training.

4.2 Inverse Model Analysis: Sampling Rare Instances Showing High Distortion in Neural Compression

Thus far, we have demonstrated that the proposed method achieves performance comparable to, or often surpassing, SOTA methods, all while remaining training-free. This unique property enables its application to fundamental sampling challenges, such as model analysis under complex importance weight functions $l(\mathbf{x})$ in high-dimensional spaces. In this section, we apply our training-free importance sampling for *inverse model analysis*, i.e., identifying samples that degrade model performance.

Application Scenarios. We consider the problem of Channel State Information (CSI) compression, where CSI represents a high-dimensional matrix—often exceeding thousands of dimen-

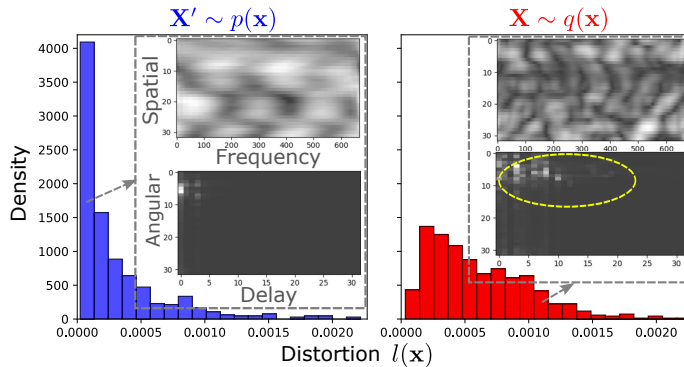


Figure 3: **Left:** Histogram of $l(\mathbf{x})$ (distortion) from $p(\mathbf{x})$ and **Right:** the importance sampling PDF $q(\mathbf{x})$ which assigns higher weights to instances with high distortion in the neural compressor. This allows rare features to be more readily observed by increasing the likelihood of sampling high-distortion instances.

sions—describing the wireless transmission link conditions between devices. Given the pivotal role of CSI in optimizing communication quality, its efficient compression and transmission have emerged as crucial challenges in wireless communication research and industrial standards [47]. Neural compressors, typically implemented as autoencoders comprising an encoder F_{enc} and a decoder F_{dec} , have been extensively studied for this purpose and continue to be an active area of research [48, 49, 50].

Importance Sampling Formulation. In real-world industrial applications, rigorous analysis of model reliability is essential. A fundamental question in this context is: *Under what conditions does our task model, i.e., the autoencoder, fail?* Importance sampling provides a principled approach to address this. By defining an importance weight function as $l(\mathbf{x}) = D(F_{\text{dec}}(F_{\text{enc}}(\mathbf{x})), \mathbf{x})$, where D denotes the distortion measure—specifically, Mean Squared Error (MSE) in this case—we can efficiently giving high importance weight to samples that exhibit high distortion, thereby identifying failure modes of the neural autoencoder model.

This approach is particularly valuable in scenarios where high-distortion samples are rare. A brute-force strategy that generates a large volume of samples, computes distortions, and applies an accept/reject procedure would be computationally inefficient. Also, traditional importance sampling methods are impractical in this setting, especially when multiple neural autoencoders need to be compared, as they necessitate training a separate generative model for each neural autoencoder under evaluation. In contrast, our training-free importance sampling method enables efficient *inverse model analysis* of neural models.

For the experiment, we utilize DDPM to obtain $\nabla_{\mathbf{x}} \log p_t(\mathbf{x})$ with CSI data from Quasi Deterministic Radio Channel Generator [51, 52]. The convolutional neural architecture-based autoencoder comprising F_{enc} and F_{dec} is trained through the dataset generated from DDPM in direction of minimizing MSE.

Results. We sample 10^4 CSI instances using both the original and importance sampling methods to measure average distortion under the neural compressor. In Fig. 3, we present the distortion

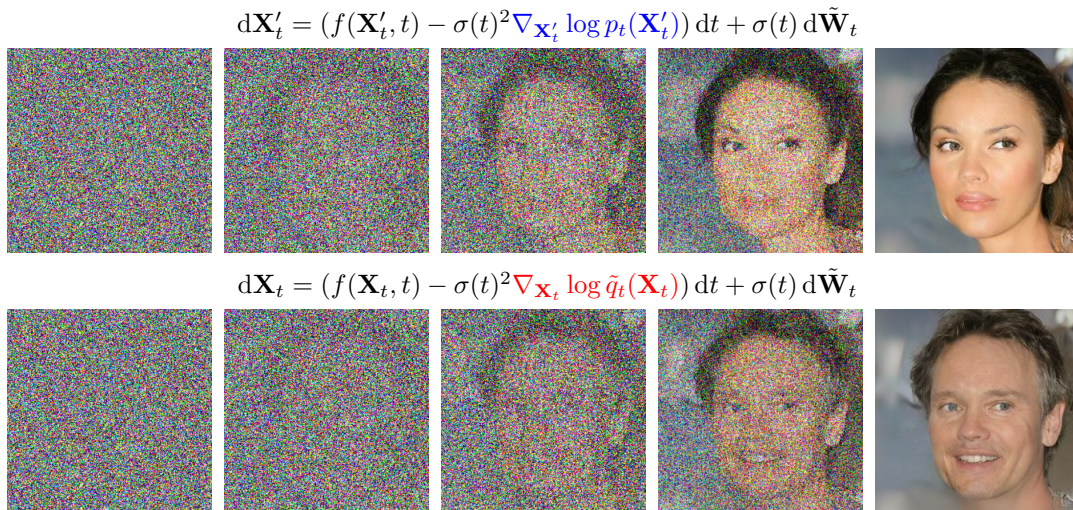


Figure 4: *Can a neural classifier serve as an importance weight in a completely training-free manner for SGM which is never trained with class information? - YES.* Our method can use any external differentiable importance weight function, e.g., a neural gender classifier.

histograms from $p(\mathbf{x})$ and $q(\mathbf{x})$. On the left-hand side, we also visualize a sample from $p(\mathbf{x})$ showing relatively small distortion of 10^{-4} in both domain spatial-frequency and angular-delay domains through inverse Fourier transform. On the right-hand side, we represent a sample from $q(\mathbf{x})$ showing compression distortion more than 10^{-3} .

The histograms show that our method effectively samples rare, high-distortion instances that are infrequent in the original distribution (e.g., cases with distortion greater than 10^{-3} occur in only 5% of samples). With importance sampling, their frequency increases to over 16%. Table 2 further demonstrates that the average distortion of importance samples in the autoencoder model, $\mathbb{E}_{\mathbf{X} \sim q}[l(\mathbf{X})]$, is nearly twice that of samples from the base distribution, $\mathbb{E}_{\mathbf{X}' \sim p}[l(\mathbf{X}')]$. This facilitates targeted feature analysis, enabling the identification of characteristics unique to rare, high-distortion samples—such as dominant scatter patterns in the angular-delay domain (highlighted by yellow dotted circles), which pose significant challenges for compression [53, 54]. In contrast, lower-distortion samples exhibit minimal scattering in the delay domain, as shown on the left.

4.3 Versatility and Scalability

One of the key advantages of our approach is its *versatility* to generate samples with varying characteristics from a given SGM. We illustrate this through the following examples: (a) *Neural classifier-driven sampling (Exp-(a))* and (b) *Sampling images with desired frequency properties from a foundation diffusion model (Exp-(b))*. Additionally, our experiments highlight the *scalability* of our approach, as we apply it to various high-dimensional data, including natural images, image-text pairings, and large-scale diffusion models such as foundational models.

Exp-(a): Neural Classifier-Driven Sampling. Consider an SGM trained without “class” awareness, such as gender, yet capable of generating celebrity-like faces (trained on CelebA [55]).

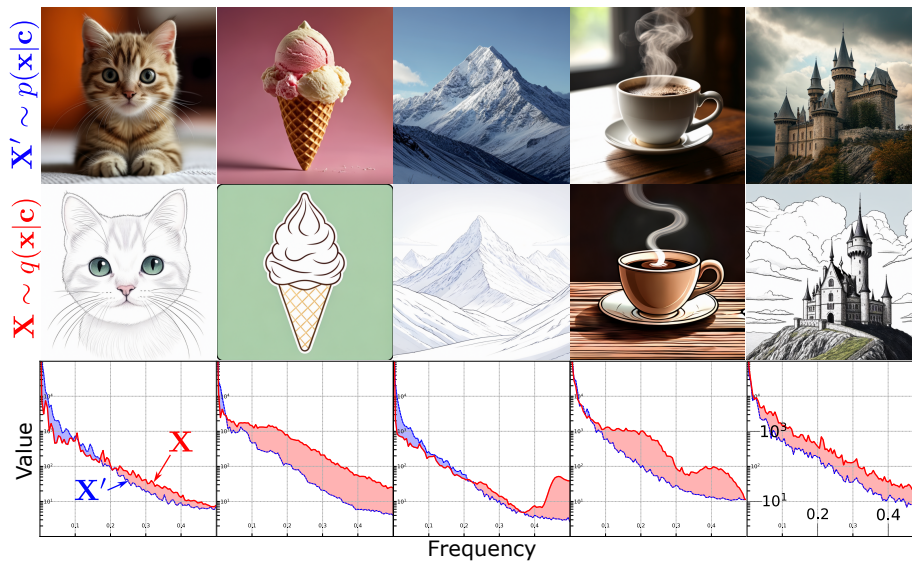


Figure 5: **First row**: Samples from $p(\mathbf{x})$, **Second row**: samples generated from $q(\mathbf{x})$. Our approach can generate samples containing elevated high-frequency components via setting $l(\mathbf{x})$ accordingly.

Now, assume an independent neural classifier can identify whether an image belongs to the “man” class. While the SGM itself is unaware of class-level information, the classifier reveals that 35% of the samples generated by the SGM are classified as “man,” implying a *high bias* in the original image distribution. *What if we want to efficiently generate more faces of “man”?*

Our method can leverage the external neural classifier as an importance weight function to adjust “man” class sampling, even without SGM’s class awareness; by setting $l(\mathbf{x})$ as the classifier’s logit for “man”, the importance sampling distribution $q(\mathbf{x})$ puts more emphasis on man-like faces.

Fig. 4 illustrates the difference between the backward diffusion process of base SGM trained over CelebA dataset (top) and the proposed backward diffusion process for importance sampling (bottom) based on the neural classifier importance weight. As shown in Table 2, our method successfully increases the sampling probability of the “man” class from 35% to 51%, achieving this without any retraining of the SGM.

Exp-(b): Sampling High-Spatial-Frequency Images from Foundation Diffusion Models.

The scalability of our proposed method makes it well-suited for application to large-scale foundation models, such as StableCascade [31], which utilize pretrained *text-conditional* score functions, $\nabla_{\mathbf{x}} \log p_t(\mathbf{x}|\mathbf{c})$, where \mathbf{c} represents the conditioning text. Our approach extends this capability to enable text-conditional importance sampling via $\nabla_{\mathbf{x}} \log q_t(\mathbf{x}|\mathbf{c})$.

This experiment demonstrates that our importance sampling can control foundation diffusion models by utilizing an externally defined importance function. Specifically, we define an importance weight function $l(\mathbf{x})$ that assigns higher values to images with pronounced high-frequency components, identified via Fourier Transform with radial masks applied to each RGB channel. As shown in Fig. 5, applying this function enables the generation of images with highly emphasized edges (bottom row) compared to general outputs (top row). Notably, this is achieved *without text-conditioning related to the characteristics of the images*. These results highlight the potential of our training-free

importance sampling method for *offering a new dimension of control beyond text prompts*.

5 Conclusion

We proposed a novel training-free score-based importance sampling methodology that models the importance sampling process as a backward diffusion process. By leveraging the score function of the base PDF and the importance weight function, our approach eliminates the need for additional training. This framework offers a scalable and efficient solution, particularly for scenarios where varying importance criteria are required. We anticipate that the proposed method will enable diverse and practical applications of importance sampling in score-based generative models, addressing challenges in adaptive sampling, bias mitigation, and model interpretation.

Impact Statement

The proposed method facilitates importance sampling with a wide range of existing pretrained score-based models and importance weight functions. We explicitly clarify that ***the primary objective of this study is to advance methodological rigor and the field of Machine Learning***; this work neither intends to advocate nor promote any particular social perspective through the experimental results presented. We do acknowledge the potential for this approach to be misused in reinforcing biased sampling practices, though, and thus strongly encourage careful consideration of the implications associated with its application.

References

- [1] J. Ho, A. Jain, and P. Abbeel, “Denoising diffusion probabilistic models,” *Advances in Neural Information Processing Systems*, vol. 33, pp. 6840–6851, 2020.
- [2] J. Song, C. Meng, and S. Ermon, “Denoising diffusion implicit models,” in *International Conference on Learning Representations*, 2021.
- [3] Y. Song, J. Sohl-Dickstein, D. P. Kingma, A. Kumar, S. Ermon, and B. Poole, “Score-based generative modeling through stochastic differential equations,” in *International Conference on Learning Representations*, 2021.
- [4] P. Dhariwal and A. Q. Nichol, “Diffusion models beat GANs on image synthesis,” in *Advances in Neural Information Processing Systems*, 2021.
- [5] A. Ramesh, M. Pavlov, G. Goh, S. Gray, C. Voss, A. Radford, M. Chen, and I. Sutskever, “Zero-shot text-to-image generation,” in *Proceedings of the 38th International Conference on Machine Learning* (M. Meila and T. Zhang, eds.), vol. 139 of *Proceedings of Machine Learning Research*, pp. 8821–8831, PMLR, 18–24 Jul 2021.
- [6] Z. Kong, W. Ping, J. Huang, K. Zhao, and B. Catanzaro, “Diffwave: A versatile diffusion model for audio synthesis,” in *International Conference on Learning Representations (ICLR)*, 2021.
- [7] N. Chen, Y. Zhang, H. Zen, R. J. Weiss, M. Norouzi, and W. Chan, “WaveGrad: Estimating gradients for waveform generation,” in *International Conference on Learning Representations (ICLR)*, 2021.
- [8] T. Lee, J. Park, H. Kim, and J. G. Andrews, “Generating high dimensional user-specific wireless channels using diffusion models.” arXiv preprint arXiv:2409.03924, 2024.
- [9] J. Zhang, S. Xu, Z. Zhang, C. Li, and L. Yang, “A denoising diffusion probabilistic model-based digital twinning of isac mimo channel,” *IEEE Internet of Things Journal*, vol. PP, no. 99, pp. 1–1, 2024.
- [10] C. P. Robert and G. Casella, *Monte Carlo Statistical Methods*. Springer Texts in Statistics, New York: Springer, 2nd ed., 2004.
- [11] J. Byrd and Z. C. Lipton, “What is the effect of importance weighting in deep learning?,” in *Proceedings of the 36th International Conference on Machine Learning*, vol. 97 of *Proceedings of Machine Learning Research*, pp. –, PMLR, June 2019.
- [12] C. Cortes, Y. Mansour, and M. Mohri, “Learning bounds for importance weighting,” in *Advances in Neural Information Processing Systems (NIPS)*, 2010.
- [13] F. Kamiran and T. Calders, “Data preprocessing techniques for classification without discrimination,” *Knowledge and Information Systems*, vol. 33, pp. 1–33, 2012.
- [14] A. Q. Nichol, P. Dhariwal, A. Ramesh, P. Shyam, P. Mishkin, B. McGrew, I. Sutskever, and M. Chen, “Glide: Towards photorealistic image generation and editing with text-guided diffusion models,” in *International Conference on Machine Learning*, pp. 16784–16804, PMLR, 2022.

- [15] D. Podell, Z. English, K. Lacey, A. Blattmann, T. Dockhorn, J. Müller, J. Penna, and R. Rombach, “Sdxl: Improving latent diffusion models for high-resolution image synthesis,” in *International Conference on Learning Representations*, 2024.
- [16] D. Kim, Y. Kim, S. J. Kwon, W. Kang, and I.-C. Moon, “Refining generative process with discriminator guidance in score-based diffusion models,” in *International Conference on Machine Learning*, pp. 16567–16598, PMLR, 2023.
- [17] L. Rout, Y. Chen, A. Kumar, C. Caramanis, S. Shakkottai, and W.-S. Chu, “Beyond first-order tweedie: Solving inverse problems using latent diffusion,” in *Proceedings of the IEEE/CVF Conference on Computer Vision and Pattern Recognition*, pp. 9472–9481, 2024.
- [18] L. Rout, N. Raoof, G. Daras, C. Caramanis, A. Dimakis, and S. Shakkottai, “Solving linear inverse problems provably via posterior sampling with latent diffusion models,” *Advances in Neural Information Processing Systems*, vol. 36, 2024.
- [19] H. Chung, J. Kim, M. T. Mccann, M. L. Klasky, and J. C. Ye, “Diffusion posterior sampling for general noisy inverse problems,” in *International Conference on Learning Representations*, 2022.
- [20] A. Doucet, W. Grathwohl, A. G. Matthews, and H. Strathmann, “Score-based diffusion meets annealed importance sampling,” *Advances in Neural Information Processing Systems*, vol. 35, pp. 21482–21494, 2022.
- [21] B. D. Anderson, “Reverse-time diffusion equation models,” *Stochastic Processes and their Applications*, vol. 12, no. 3, pp. 313–326, 1982.
- [22] A. Lugmayr, M. Danelljan, A. Romero, F. Yu, R. Timofte, and L. Van Gool, “Repaint: Inpainting using denoising diffusion probabilistic models,” in *Proceedings of the IEEE/CVF conference on computer vision and pattern recognition*, pp. 11461–11471, 2022.
- [23] A. Q. Nichol and P. Dhariwal, “Improved denoising diffusion probabilistic models,” in *International conference on machine learning*, pp. 8162–8171, PMLR, 2021.
- [24] J. Choi, S. Kim, Y. Jeong, Y. Gwon, and S. Yoon, “Ilvr: Conditioning method for denoising diffusion probabilistic models,” *arXiv preprint arXiv:2108.02938*, 2021.
- [25] J. V. Beck, K. D. Cole, A. Haji-Sheikh, and B. Litkouhl, *Heat conduction using Green’s function*. Taylor & Francis, 1992.
- [26] D. G. Duffy, *Green’s functions with applications*. Chapman and Hall/CRC, 2015.
- [27] E. N. Economou, *Green’s functions in quantum physics*, vol. 7. Springer Science & Business Media, 2006.
- [28] B. Efron, “Tweedie’s formula and selection bias,” *Journal of the American Statistical Association*, vol. 106, no. 496, pp. 1602–1614, 2011.
- [29] K. Kim and J. C. Ye, “Noise2score: tweedie’s approach to self-supervised image denoising without clean images,” *Advances in Neural Information Processing Systems*, vol. 34, pp. 864–874, 2021.
- [30] P. E. Kloeden, E. Platen, P. E. Kloeden, and E. Platen, *Stochastic differential equations*. Springer, 1992.
- [31] P. Pernias, D. Rampas, M. L. Richter, C. Pal, and M. Aubreville, “Würstchen: An efficient architecture for large-scale text-to-image diffusion models,” in *The Twelfth International Conference on Learning Representations*, 2024.
- [32] R. Rombach, A. Blattmann, D. Lorenz, P. Esser, and B. Ommer, “High-resolution image synthesis with latent diffusion models,” in *Proceedings of the IEEE/CVF conference on computer vision and pattern recognition*, pp. 10684–10695, 2022.

- [33] H. Chen, H. Lee, and J. Lu, “Improved analysis of score-based generative modeling: User-friendly bounds under minimal smoothness assumptions,” in *International Conference on Machine Learning*, pp. 4735–4763, PMLR, 2023.
- [34] V. De Bortoli, “Convergence of denoising diffusion models under the manifold hypothesis,” *Transactions on Machine Learning Research*, 2022.
- [35] S. Chen, S. Chewi, J. Li, Y. Li, A. Salim, and A. Zhang, “Sampling is as easy as learning the score: theory for diffusion models with minimal data assumptions,” in *The Eleventh International Conference on Learning Representations*, 2023.
- [36] V. De Bortoli, J. Thornton, J. Heng, and A. Doucet, “Diffusion schrödinger bridge with applications to score-based generative modeling,” *Advances in Neural Information Processing Systems*, vol. 34, pp. 17695–17709, 2021.
- [37] Z. I. Botev, D. P. Kroese, R. Y. Rubinstein, and P. L’Ecuyer, “The cross-entropy method for optimization,” in *Handbook of statistics*, vol. 31, pp. 35–59, Elsevier, 2013.
- [38] W. Grathwohl, R. T. Chen, J. Bettencourt, and D. Duvenaud, “Scalable reversible generative models with free-form continuous dynamics,” in *International Conference on Learning Representations*, p. 7, 2019.
- [39] Y. Perugachi-Diaz, J. Tomczak, and S. Bhulai, “Invertible densenets with concatenated lipswish,” *Advances in Neural Information Processing Systems*, vol. 34, pp. 17246–17257, 2021.
- [40] D. M. Endres and J. E. Schindelin, “A new metric for probability distributions,” *IEEE Transactions on Information theory*, vol. 49, no. 7, pp. 1858–1860, 2003.
- [41] M. Germain, K. Gregor, I. Murray, and H. Larochelle, “Made: Masked autoencoder for distribution estimation,” in *International conference on machine learning*, pp. 881–889, PMLR, 2015.
- [42] G. Papamakarios, T. Pavlakou, and I. Murray, “Masked autoregressive flow for density estimation,” *Advances in neural information processing systems*, vol. 30, 2017.
- [43] T. Müller, B. McWilliams, F. Rousselle, M. Gross, and J. Novák, “Neural importance sampling,” *ACM Transactions on Graphics (ToG)*, vol. 38, no. 5, pp. 1–19, 2019.
- [44] C. Durkan, A. Bekasov, I. Murray, and G. Papamakarios, “Neural spline flows,” *Advances in neural information processing systems*, vol. 32, 2019.
- [45] C. Durkan, A. Bekasov, I. Murray, and G. Papamakarios, “Cubic-spline flows,” in *ICML Workshop on Invertible Neural Nets and Normalizing Flows*, 2019.
- [46] M. Patocchiola, A. Shysheya, K. Hofmann, and R. E. Turner, “Transformer neural autoregressive flows,” in *ICML 2024 Workshop on Structured Probabilistic Inference & Generative Modeling*, 2024.
- [47] X. Lin, “An overview of 5g advanced evolution in 3gpp release 18,” *IEEE Communications Standards Magazine*, vol. 6, no. 3, pp. 77–83, 2022.
- [48] J. Guo, C.-K. Wen, S. Jin, and G. Y. Li, “Overview of deep learning-based csi feedback in massive mimo systems,” *IEEE Transactions on Communications*, vol. 70, no. 12, pp. 8017–8045, 2022.
- [49] S. Jiang and A. Alkhateeb, “Digital Twin Aided Massive MIMO: CSI Compression and Feedback,” in *IEEE International Conference on Communications*, (Denver, CO, USA), pp. 1–6, IEEE, June 2024.
- [50] Z. Qin, L. Liang, Z. Wang, S. Jin, X. Tao, and W. Tong, “AI Empowered Wireless Communications: From Bits to Semantics,” *Proceedings of the IEEE*, vol. 112, pp. 621–652, July 2024.
- [51] S. Jaeckel et al., “Quadriga: A 3-d multi-cell channel model with time evolution for enabling virtual field trials,” *IEEE transactions on antennas and propagation*, vol. 62, no. 6, pp. 3242–3256, 2014.
- [52] S. Jaeckel et al., “Quadriga - quasi deterministic radio channel generator, user manual and documentation,” *Fraunhofer Heinrich Hertz Institute*, vol. 2.6.1, 2021.

- [53] C.-K. Wen, W.-T. Shih, and S. Jin, "Deep learning for massive mimo csi feedback," *IEEE Wireless Communications Letters*, vol. 7, no. 5, pp. 748–751, 2018.
- [54] H. Kim, H. Kim, and G. De Veciana, "Learning variable-rate codes for csi feedback," in *GLOBECOM 2022-2022 IEEE Global Communications Conference*, pp. 1435–1441, IEEE, 2022.
- [55] Z. Liu, P. Luo, X. Wang, and X. Tang, "Deep learning face attributes in the wild," in *Proceedings of the IEEE International Conference on Computer Vision (ICCV)*, pp. 3730–3738, 2015.